Phase diagram of graphene nanoribbons and band-gap bifurcation of Dirac fermions under quantum confinement

Y. Y. Sun,[1] W. Y. Ruan,[2] Xingfa Gao,[1] Junhyeok Bang,[1] Yong-Hyun Kim,[3] Kyuho Lee,[4] D. West,[1] Xin Liu,[1] T.-L. Chan,[1] M. Y. Chou,[2,5,*] and S. B. Zhang[1,†]

[1]*Department of Physics, Applied Physics, and Astronomy, Rensselaer Polytechnic Institute, Troy, New York 12180, USA*

[2]*School of Physics, Georgia Institute of Technology, Atlanta, Georgia 30332, USA*

[3]*Graduate School of Nanoscience and Technology (WCU) and KAIST Institute for the NanoCentury, KAIST, Daejeon 305-701, Korea*

[4]*Department of Physics and Astronomy, Rutgers University, Piscataway, New Jersey 08854, USA*

[5]*Institute of Atomic and Molecular Sciences, Academia Sinica, Taipei 10617, Taiwan*

(Received 21 April 2011; revised manuscript received 14 May 2012; published 30 May 2012)

A p-T phase diagram of graphene nanoribbons (GNRs) terminated by hydrogen atoms is established based on first-principles calculations, where the stable phase at standard conditions (25 °C and 1 bar) is found to be a zigzag GNR (zzGNR). The stability of this new GNR is understood based on an electron-counting model, which predicts semiconducting nonmagnetic zzGNRs. Quantum confinement of Dirac fermions in the stable zzGNRs is found to be qualitatively different from that in ordinary semiconductors. Bifurcation of the band gap is predicted to take place, leading to the formation of polymorphs with distinct band gaps but equal thermodynamic stability. A tight-binding model analysis reveals the role of edge symmetry on the band-gap bifurcation.

DOI: 10.1103/PhysRevB.85.195464 PACS number(s): 73.22.−f, 73.22.Pr, 61.48.Gh, 81.65.Rv

I. INTRODUCTION

Graphene, as a Dirac fermion system, possesses extremely high carrier mobilities[1] and has been envisaged as an electronic material candidate for the postsilicon era.[2] Perfect graphene, however, is a semimetal with a zero electronic band gap. In this regard, graphene nanoribbons (GNRs) have attracted considerable attention[3–8] because they could be made semiconducting with band gaps opened by the quantum confinement effect. In recent years, a number of techniques have been developed to produce GNRs.[7–11] Prototypical electric-circuit elements such as field-effect transistors based on GNRs have also been demonstrated experimentally.[6,12]

The electronic properties of GNRs are governed by several factors, such as chirality, ribbon width, and atomic structure at the two edges. The effect of the chirality has been studied.[3,4,13] An inverse dependence of the band gap on the ribbon width has also been established.[4] The understanding of the edge effects has so far focused on the disorder at the edges.[14–20] Such edge disorder introduces localized gap states that dominate electron transport in the GNRs. In the past several years, significant progress has been made to produce higher-quality GNRs by, e.g., solution-phase fabrication,[8] bottom-up synthesis,[9] carbon nanotube unzipping,[10,11,21,22] Joule heating,[23] and nanowire-masked lithography.[24] Atomically smooth edges enable precise control on the electronic properties of GNRs for nanoelectronics. Meanwhile, a new physics of Dirac fermions under quantum confinement that are shadowed by the edge disorder effects is expected to emerge in the GNRs with atomically smooth edges.

In this paper, we address, by first-principles calculations, two fundamental issues regarding GNRs: (1) the thermodynamic phase diagram upon edge hydrogenation and (2) the quantum confinement of Dirac fermions and its explicit edge dependence. The first issue is important because for the physical properties of a batch of GNRs thermodynamics is expected to play an important role, whereas the second issue is important because there is no *a priori* knowledge that quantum confinement of Dirac fermions should obey the same physics as that in ordinary semiconductors. Concerning issue (1), we propose a new H-passivated pattern of the zigzag (zz) GNRs. It changes the relative thermodynamic stability between the armchair (ac) GNR and zzGNR known in the literature,[25] making the latter more stable under the standard conditions (1 bar and 300 K). Concerning issue (2), we show that quantum confinement of Dirac fermions, as demonstrated in the stable zzGNR, is fundamentally different from that in ordinary semiconductors. The symmetric band structure between electrons and holes near the degenerate K point in the Brillouin zone of the same atomic character, namely, carbon π states, makes it possible to mix the electron and hole states upon size confinement with little energy penalty. As such, two sets of zzGNRs with equal stability but drastically different band gaps emerge, with a nearly constant gap ratio of about 2.8. It suggests that uncertainty of the band gaps of zzGNRs could be an intrinsic property of the Dirac fermions under quantum confinement.

II. COMPUTATIONAL METHOD

Our first-principles calculations were based on spin-polarized density functional theory with the Perdew-Burke-Ernzerhof approximation[26] to the exchange-correlation functional. The core-valence interactions were described by the projector augmented-wave potentials[27] as implemented in the VASP code.[28] Plane waves with a kinetic energy cutoff of 544 eV were used as the basis set. The calculations were carried out in periodic supercells, where the GNRs from neighboring supercells were separated by at least 10 Å. All atoms were relaxed until the forces were smaller than 0.01 eV/Å. The length of the lattice vector, L, along the periodic direction was optimized until the stress was smaller than 1 kbar. A $1 \times 4 \times 1$ (or $1 \times 8 \times 1$ for a reduced cell) k-point set was used for the Brillouin zone integration.

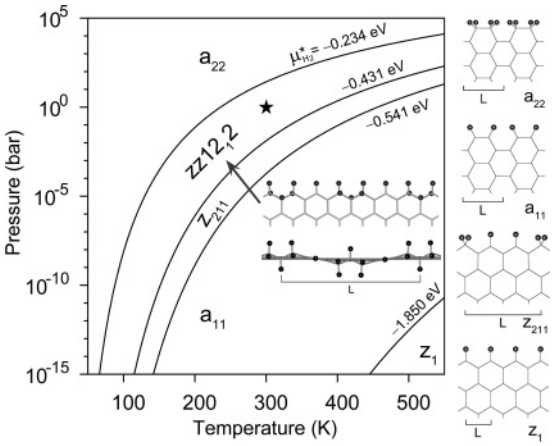

FIG. 1. Phase diagram of hydrogen-passivated GNRs with both zz and ac edges. The insets show the atomic structures of the corresponding passivation patterns. The star marks the standard atmospheric conditions ($T = 300$ K and $P = 1$ bar). The values of $\mu^*_{H_2}$ in Eq. (2) at the phase boundaries are also given. L is the length of the lattice vector.

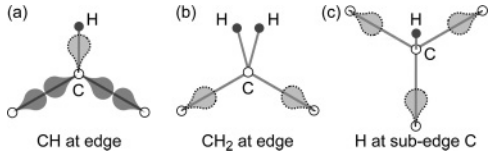

FIG. 2. Schematic showing the dangling p_z electrons at three types of C sites near the zz edge: (a) edge C bonded with a single H atom, (b) edge C bonded with double H atoms, and (c) subedge C bonded with a single H atom. Each teardrop-shaped lobe represents one third of the p_z electrons. The darker lobes represent the p_z electrons participating in the resonant bonding with the rest of the system, while the brighter lobes with dashed outlines represent dangling p_z electrons.

III. PHASE DIAGARAM OF GRAPHENE NANORIBBONS

Figure 1 shows the calculated phase diagram of hydrogen-passivated GNRs with either zz or ac edges. We compare the thermodynamic stability of the various GNRs by their edge energy,

$$\Delta G = [E_{\mathrm{GNR}} - N_{\mathrm{C}} E_{\mathrm{C}} - N_{\mathrm{H}} \mu_{\mathrm{H}}]/2L, \tag{1}$$

where E_{GNR} is the total energy of a GNR, N_{C} and N_{H} are the numbers of C and H atoms, respectively, E_{C} is the total energy per C atom in graphene, and μ_{H} is the chemical potential of H in equilibrium with H_2 gas. μ_{H} is related to temperature T and pressure P by[25,29]

$$\begin{aligned}\mu_{\mathrm{H}}(T,P) &= \frac{1}{2}\Big[E_{\mathrm{H_2}} + H^\circ(T) - H^\circ(0) \\ &\quad - TS^\circ(T) + k_{\mathrm{B}}T \ln\left(\frac{P}{P^\circ}\right)\Big] \\ &\equiv \frac{1}{2}\big[E_{\mathrm{H_2}} + \mu^*_{\mathrm{H_2}}(T,P)\big],\end{aligned} \tag{2}$$

where $E_{\mathrm{H_2}}$ is the total energy of a free H_2 molecule and H° and S° are the enthalpy and entropy, respectively, of H_2 gas at $P^\circ = 1$ bar, which are obtained from a standard database.[30] The most significant result in Fig. 1 is the $zz12_12$ structure that maximizes the aromaticity in the interior of the graphene sheet. The inset in Fig. 1 shows the atomic structure for $zz12_12$, where every third C atom at the edge is passivated by a single H atom, while others are passivated by two H atoms. In addition, there is a subedge C atom that is also bonded to a H atom, in contrast to any known model. Previous calculation indicates that the ac edges are more stable than the zz edges. However, with the new $zz12_12$ structure, the reverse is true. Figure 1 shows that at or near standard conditions (25 °C and 1 bar), $zz12_12$ is the most stable edge structure. Our results are thus consistent with the repeatedly observed zz edges of graphene in various experimental conditions.[23,31–34] It is interesting to note that a recent theoretical simulation of x-ray absorption spectra[35] suggests that three extrinsic features observed in the graphene systems in a number of experiments are the results of mixed C-H and C-H_2 motifs at the edge and subedge C sites that are consistent with our model.

IV. ELECTRON-COUNTING MODEL FOR ZIGZAG GRAPHENE NANORIBBONS

The stability of the $zz12_12$ edge can be understood based on the following electron-counting model. In bulk graphene, each carbon site contributes one p_z electron to the resonant π bonding. One can consider that each C atom shares 1/3 p_z electrons with each of its three neighbors. At a z_1 edge (see Fig. 1), each H atom saturates a dangling σ bond on an edge C atom (on the A sublattice of graphene, for example), while 1/3 p_z electrons become "dangling," as illustrated in Fig. 2(a). This results in unequal numbers of π electrons on the A and B sublattices. Similarly, as illustrated in Figs. 2(b) and 2(c), attaching two H atoms to an edge C atom creates 1/3 dangling p_z electrons on each of the two neighboring C atoms (on the B sublattice), while attaching one H atom to a subedge C atom (on the B sublattice) will create 1/3 dangling p_z electrons on each of the three neighboring C atoms (on the A sublattice). With the above electron-counting model, our extensive first-principles calculations establish the rule that if the dangling π electrons on the A and B sublattices are equal, the edge structure will not exhibit metallic edge states or localized magnetic moments. In general, semiconducting edges are more stable than metallic edges. Among all possible edge structures with the unit-cell length smaller than $3L(z_1)$, only four edges, namely, z_{211}, $zz12_12$, $zz1_122$, and $zz2_12_12$, satisfy the rule, although the latter two are less stable and hence do not appear in the phase diagram in Fig. 1. It is interesting to note that, to satisfy the electron-counting rule, the unit-cell length has to be a multiple of $3L(z_1)$.

V. BAND-GAP BIFURCATION

Because of the triple period of the stable zzGNRs, an interesting issue arises; that is, if both edges are $zz12_12$, there would be four inequivalent registries of the two edges. Here, we only need to consider two inequivalent registries in a half cell, as the consideration of the full cell does not yield any new physics except that the edge energy of the full cell is about 6 meV/Å lower than that of the half cell. The two registries,

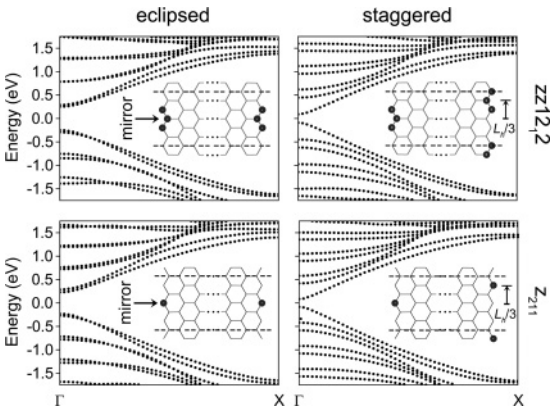

FIG. 3. Band structures of (left) eclipsed and (right) staggered polymorphs of zzGNRs with (top) zz12$_1$2 and (bottom) z_{211} passivations. The ribbon width N is 16. The energy zero is selected at the middle of the band gap. Insets show the respective atomic structures, where the dashed lines define the unit cells. The mirror symmetry present in the eclipsed polymorph is marked by an arrow. The registry shift of the two edges in the staggered polymorph by $L_h/3$ is illustrated in the insets. L_h is one half of L in Fig. 1. For clarity, H atoms are not shown. Instead, the sp^3 C atoms are highlighted by black spheres.

named *eclipsed* and *staggered* polymorphs, are shown in the insets of Fig. 3. The two polymorphs differ by a registry shift of the passivation hydrogen at the two edges with respect to each other by $L_h/3$. Note that the lattice vector L_h for zz12$_1$2 in Fig. 3 is only one half of the L in Fig. 1.

As expected, the band gaps of the polymorphs follow a linear relation, $E_g = \alpha/W$,[4,8] as shown in Fig. 4, where the ribbon width W is given by $(3N/2 - 1)d_{C-C}$ with N being the number of zz rows and d_{C-C} being the calculated C-C bond length in graphene (1.425 Å). Figure 3, however, reveals that the two polymorphs have drastically different band structures. In particular, the E_g ratio γ is nearly a constant of about

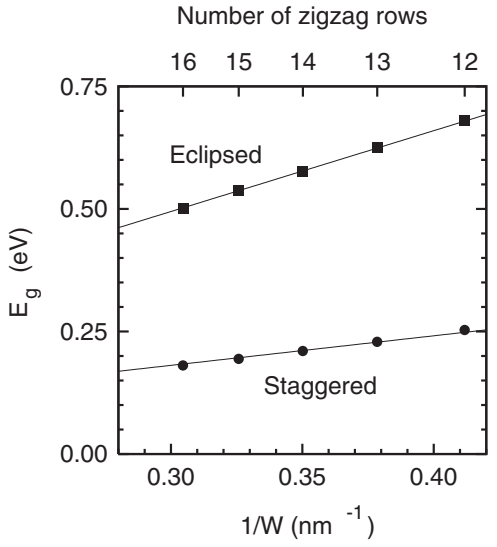

FIG. 4. Band gaps of the two zzGNR polymorphs with zz12$_1$2 passivation as a function of the inverse ribbon width $1/W$ and the number of zz rows N. Solid lines are linear fits with $\alpha = 1.65$ and 0.60 eV nm, respectively, for the eclipsed and staggered polymorphs.

TABLE I. Calculated band gaps (in eV) and their ratio γ for the two polymorphs of zzGNRs with $N = 16$ and different edge passivations. The zzHO$_H$O and z_{OHH} patterns are modified zz12$_1$2 and z_{211}, respectively, by replacing every two same-site H atoms with a single O atom. Also given are the edge energy differences between the two polymorphs, $d(\Delta G)$, in meV/Å.

	zz12$_1$2	zzHO$_H$O	z_{211}	z_{OHH}	$z(600)_{1111}$
Eclipsed	0.500	0.412	0.458	0.313	0.546
Staggered	0.181	0.187	0.169	0.135	0.187
γ	2.76	2.20	2.72	2.32	2.92
$d(\Delta G)$	0.24	0.23	0.19	0.13	0.33

2.8 with respect to W, as seen in Fig. 4. More importantly, the difference in the edge energy ΔG of the two polymorphs converges with respect to W quickly to zero. For example, for $N = 16$, the calculated difference in ΔG is only 0.24 meV/Å, as shown in Table I. This suggests a bifurcation of the Dirac fermion band gap upon quantum confinement with equal thermodynamic stability and is in sharp contrast to that of ordinary semiconductors where a single and hence definitive band gap is often obtained.

VI. TIGHT-BINDING ANALYSIS

To understand the salient physics of quantum confinement on Dirac fermions, here we present a tight-binding analysis. We start with the z_1 edges which have single periodicity (and hence no polymorphs) and exhibit an intrinsic band gap at the folded Dirac K point[36] (and a closed gap away from K due to edge states,[13] which is unimportant to the current discussion). The eigenfunctions of the Hamiltonian H_0 can be expressed as the superposition of two Bloch waves with momenta $(q_x, \pm q_y)$ in bulk graphene, where q_x is in the periodic direction of the zzGNR and q_y is quantized to satisfy the hard-wall boundary conditions. For $N \gg 1$ and $q_x = K$, the corresponding eigenvalues for the low-lying states (i.e., $n \ll N$) are doubly degenerate and are given by

$$\varepsilon_n = \frac{\pi t}{N}\left(n + \frac{1}{2}\right), \tag{3}$$

with quantum number $n = (0, \pm 1, \pm 2, \ldots)$, where t is the hopping energy between the A and B sublattices of graphene. The equal level spacing exhibited in Eq. (3) is a general property of massless Dirac fermions arising from the linear $E(q)$ dispersion.

The Hamiltonian of a zzGNR with modified edges from the z_1 can be written as $H = H_0 + \lambda V$, where λV is the on-site energy representing the effect of the extra H atoms that convert the attached C atoms from sp^2 to sp^3. V is a diagonal matrix with $V_{ii} = 0$ (or 1) if the ith C atom has the configuration of sp^2 (or sp^3), and λ is the strength of the potential that can vary from 0 to ∞. In case where an extra H atom completely removes a carbon p_z orbital from the π-electron Hamiltonian, λ goes to ∞. The eigenstates of H, $\{\Psi_n\}$, can be expressed in terms of the eigenstates of H_0, $\{\varphi_n\}$. Due to the properties of the Dirac fermions, it can be shown that Ψ_n takes on the peculiar form $\Psi_n = \sum_m F(m-n)\varphi_m$, where the expansion coefficients depend solely on the *difference* between m and

n. The functional form of F is independent of t and N in the limit $N \gg 1$. However, F depends sensitively on the symmetry of the eigenstates. There are two relevant types of symmetry: one is the mirror reflection $\boldsymbol{\sigma}$, as shown in Fig. 3, and the other is the exchange $\boldsymbol{P}$ of A and B sublattices, which can be realized by a rotation of π around a normal axis to the graphene sheet followed by an N-dependent fractional translation. If the system is invariant under the operation of $\boldsymbol{\sigma}$, as in the case of an eclipsed polymorph, one can show that $F(m) = \sigma F(-m)$, where $\sigma = \pm 1$. If the $\boldsymbol{\sigma}$ symmetry is broken, as in the case of a staggered polymorph, however, $|F(m)| \neq |F(-m)|$.

Now, consider the $\lambda \to \infty$ limit. Because the wave functions $\{\Psi_n\}$ vanish at an sp^3 site, the expectation value of V vanishes accordingly, i.e., $\langle \Psi_n | V | \Psi_n \rangle = 0$. Thus, the eigenvalues of H can be expressed by

$$E_n = \langle \Psi_n | H | \Psi_n \rangle = \langle \Psi_n | H_0 | \Psi_n \rangle = \sum_m |F(m-n)|^2 \varepsilon_m = \varepsilon_n - \frac{\pi t}{N}\beta, \tag{4}$$

where ε_n is given by Eq. (3) and $\beta \equiv \sum_m |F(m)|^2 m$ is independent of the quantum number n but dependent on the symmetry. This indicates that the effect of V is to shift all eigenstates of the same symmetry by the same amount while maintaining their energy spacing. For the eclipsed polymorph with the $\boldsymbol{\sigma}$ symmetry, $\beta = 0$ for states with both $\sigma = +1$ and -1 because $|F(m)| = |F(-m)|$. Hence its energy band gap $\frac{\pi t}{N}$ is identical to the intrinsic band gap of z_1 at $q_x = K$ if the finite-size effect of order $1/N^2$ is ignored. For the staggered polymorph, the broken $\boldsymbol{\sigma}$ symmetry leads to a nonvanishing β. Our tight-binding calculation in the limit $N \to \infty$ yields $\beta_+ \approx 1/3$ for the states that are invariant under the operation of $\boldsymbol{P}$ (e.g., the conduction band minimum (CBM) state). For the states that change their sign under the operation of $\boldsymbol{P}$ (e.g., the means valence band maximum (VBM) state), we have $\beta_- = -\beta_+$ because of the electron-hole symmetry of the Dirac fermions. The energy gap is thus given by $E_g = \frac{\pi t}{N}(1 - 2|\beta_+|) \approx \frac{\pi t}{3N}$. Hence, a nonvanishing β leads to the band gap narrowing in the staggered polymorph. In the limit of $\lambda \to \infty$ and $N \gg 1$, the ratio γ between the energy gaps of the eclipsed and staggered polymorphs is 3. As a comparison, our DFT results for $12 \leqslant N \leqslant 16$ give a value of about 2.8 for the $zz12_12$ GNRs (see Fig. 4).

VII. OTHER PASSIVATIONS

The edge effect is intrinsic to Dirac fermions and hence should not vanish due to different passivation. This is clearly true if we compare $zz12_12$ with z_{211} as γ is only changed by 1.7% (see Table I). The electronic structures are also very similar, as shown in Fig. 3. To demonstrate the universality further, we consider copassivation of the edges by H and O atoms, which can be realized by replacing every two H atoms that are bonded to a single sp^3 C atom by a single O atom. This yields from $zz12_12$ the passivation pattern $zzHO_HO$ and from z_{211} the pattern z_{OHH}. The results are listed in Table I. It can be seen that replacing two H atoms by one O atom tends to reduce γ modestly, owing to the possibly secondary effect that affects the exact value of λ. Finally, $z(600)_{1111}$,[25] with the removal of sp^3 carbon atoms, resembles $\lambda \to \infty$ and, as expected, has the largest $\gamma = 2.92$.

VIII. CONCLUSIONS

In summary, using first-principles calculations we establish the phase diagram of hydrogen-terminated GNRs, which emphasizes the importance of zigzag GNRs under standard conditions. We reveal the distinct physics of Dirac fermions under quantum confinement in the stable zzGNRs, namely, the bifurcation of band gap with equal thermodynamic stability. Our tight-binding model analysis demonstrates that the symmetry of passivating atoms at the edges determines the band gaps of the zzGNRs. We expect the band-gap bifurcation to be experimentally observed in the zzGNRs terminated by hydrogen as well as other species.

ACKNOWLEDGMENTS

W.Y.R. and M.Y.C. acknowledge support from the US Department of Energy, Office of Basic Energy Sciences, Division of Materials Sciences and Engineering, under Award No. DEFG02-97ER45632. The work at RPI was supported by the NSF (Grant No. DMR-1104994) and the DOE (Grant No. DE-SC0002623). X.G. was partially supported by the China MOST 973 program (Grant No. 2012CB934001). The supercomputer time was provided by NERSC under US DOE Grant No. DE-AC02-05CH11231 and CCNI at RPI.

*meiyin.chou@physics.gatech.edu
†zhangs9@rpi.edu

[1] K. S. Novoselov, A. K. Geim, S. V. Morozov, D. Jiang, Y. Zhang, S. V. Dubonos, I. V. Grigorieva, and A. A. Firsov, Science **306**, 666 (2004).
[2] A. K. Geim and K. S. Novoselov, Nat. Mater. **6**, 183 (2007).
[3] V. Barone, O. Hod, and G. E. Scuseria, Nano Lett. **6**, 2748 (2006).
[4] Y. W. Son, M. L. Cohen, and S. G. Louie, Phys. Rev. Lett. **97**, 216803 (2006).
[5] L. Yang, C. H. Park, Y. W. Son, M. L. Cohen, and S. G. Louie, Phys. Rev. Lett. **99**, 186801 (2007).
[6] X. R. Wang, Y. J. Ouyang, X. L. Li, H. L. Wang, J. Guo, and H. J. Dai, Phys. Rev. Lett. **100**, 206803 (2008).
[7] M. Y. Han, B. Ozyilmaz, Y. B. Zhang, and P. Kim, Phys. Rev. Lett. **98**, 206805 (2007).
[8] X. L. Li, X. R. Wang, L. Zhang, S. W. Lee, and H. J. Dai, Science **319**, 1229 (2008).
[9] J. Cai, P. Ruffieux, R. Jaafar, M. Bieri, T. Braun, S. Blankenburg, M. Muoth, A. P. Seitsonen, M. Saleh, X. Feng, K. Müllen, and R. Fasel, Nature (London) **466**, 470 (2010).
[10] L. Y. Jiao, L. Zhang, X. R. Wang, G. Diankov, and H. J. Dai, Nature (London) **458**, 877 (2009).
[11] D. V. Kosynkin, A. L. Higginbotham, A. Sinitskii, J. R. Lomeda, A. Dimiev, B. K. Price, and J. M. Tour, Nature (London) **458**, 872 (2009).
[12] L. Liao, J. W. Bai, R. Cheng, Y.-C. Lin, S. Jiang, Y. Huang, and X. F. Duan, Nano Lett. **10**, 1917 (2010).

[13]K. Nakada, M. Fujita, G. Dresselhaus, and M. S. Dresselhaus, Phys. Rev. B **54**, 17954 (1996).
[14]Y. Yoon and J. Guo, Appl. Phys. Lett. **91**, 073103 (2007).
[15]D. Querlioz, Y. Apertet, A. Valentin, K. Huet, A. Bournel, S. Galdin-Retailleau, and P. Dollfus, Appl. Phys. Lett. **92**, 042108 (2008).
[16]P. Gallagher, K. Todd, and D. Goldhaber-Gordon, Phys. Rev. B **81**, 115409 (2010).
[17]M. Y. Han, J. C. Brant, and P. Kim, Phys. Rev. Lett. **104**, 056801 (2010).
[18]K. Wakabayashi, Y. Takane, and M. Sigrist, Phys. Rev. Lett. **99**, 036601 (2007).
[19]C. Stampfer, J. Güttinger, S. Hellmüller, F. Molitor, K. Ensslin, and T. Ihn, Phys. Rev. Lett. **102**, 056403 (2009).
[20]I. Martin and Y. M. Blanter, Phys. Rev. B **79**, 235132 (2009).
[21]L. Y. Jiao, X. R. Wang, G. Diankov, H. L. Wang, and H. J. Dai, Nat. Nanotechnol. **5**, 321 (2010).
[22]A. L. Elías, A. R. Botello-Méndez, D. Meneses-Rodríguez, V. J. González, D. Ramírez-González, L. Ci, E. Muñoz-Sandoval, P. M. Ajayan, H. Terrones, and M. Terrones, Nano Lett. **10**, 366 (2010).
[23]X. Jia, M. Hofmann, V. Meunier, B. G. Sumpter, J. Campos-Delgado, J. M. Romo-Herrera, H. Son, Y.-P. Hsieh, A. Reina, J. Kong, M. Terrones, and M. S. Dresselhaus, Science **323**, 1701 (2009).
[24]J. W. Bai, X. F. Duan, and Y. Huang, Nano Lett. **9**, 2083 (2009).
[25]T. Wassmann, A. P. Seitsonen, A. M. Saitta, M. Lazzeri, and F. Mauri, Phys. Rev. Lett. **101**, 096402 (2008).
[26]J. P. Perdew, K. Burke, and M. Ernzerhof, Phys. Rev. Lett. **77**, 3865 (1996).
[27]G. Kresse and D. Joubert, Phys. Rev. B **59**, 1758 (1999).
[28]G. Kresse and J. Furthmüller, Comput. Mater. Sci. **6**, 15 (1996).
[29]K. Reuter and M. Scheffler, Phys. Rev. B **65**, 035406 (2001).
[30]The NIST Chemistry WebBook, [http://webbook.nist.gov/].
[31]K. A. Ritter and J. W. Lyding, Nat. Mater. **8**, 235 (2009).
[32]C. Ö. Girit, J. C. Meyer, R. Erni, M. D. Rossell, C. Kisielowski, L. Yang, C.-H. Park, M. F. Crommie, M. L. Cohen, S. G. Louie, and A. Zettl, Science **323**, 1705 (2009).
[33]J. H. Warner, M. H. Rümmeli, L. Ge, T. Gemming, B. Montanari, N. M. Harrison, B. Büchner, and G. A. D. Briggs, Nat. Nanotechnol. **4**, 500 (2009).
[34]B. Krauss, P. Nemes-Incze, V. Skakalova, L. P. Biro, K. von Klitzing, and J. H. Smet, Nano Lett. **10**, 4544 (2010).
[35]Z. Hou, X. Wang, T. Ikeda, S.-F. Huang, K. Terakura, M. Boero, M. Oshima, M. Kakimoto, and S. Miyata, J. Phys. Chem. C **115**, 5392 (2011).
[36]The Dirac K point of graphene is folded to a point at $2/3\ \Gamma$-X and to the Γ point for zzGNRs with z_1 and zz$12_1$2 edges, respectively.